

See discussions, stats, and author profiles for this publication at: <https://www.researchgate.net/publication/228580100>

# Structure Determination of Trialanine in Water Using Polarization Sensitive Two-Dimensional Vibrational Spectroscopy

ARTICLE *in* THE JOURNAL OF PHYSICAL CHEMISTRY B · NOVEMBER 2000

Impact Factor: 3.3 · DOI: 10.1021/jp001546a

---

CITATIONS

276

---

READS

66

2 AUTHORS, INCLUDING:



Sander Woutersen

University of Amsterdam

103 PUBLICATIONS 4,303 CITATIONS

SEE PROFILE

# Structure Determination of Trialanine in Water Using Polarization Sensitive Two-Dimensional Vibrational Spectroscopy

S. Woutersen and P. Hamm\*

Max-Born-Institut für Nichtlineare Optik und Kurzzeitspektroskopie, Max-Born-Strasse 2A, D-12489 Berlin, Germany

Received: April 24, 2000; In Final Form: July 24, 2000

Using polarization sensitive two-dimensional (2D) vibrational spectroscopy on the amide I mode, the central backbone structure of trialanine in aqueous solution is investigated. We exploit the polarization sensitivity of the 2D pump–probe signal to reveal the cross-peak structure hidden under the strong diagonal peaks. The dihedral angles  $\phi$  and  $\psi$  characterizing the peptide backbone structure are derived directly from the cross-peak intensity and anisotropy, demonstrating the potential of 2D spectroscopy as a tool for peptide structure elucidation.

## I. Introduction

Recent experiments have shown that the two-dimensional (2D) vibrational spectrum of the amide I band of small peptides is determined mainly by their secondary structure.<sup>1</sup> The secondary structure of a peptide determines the relative positions and orientations its peptide ( $-\text{CO}-\text{NH}-$ ) groups, and hence the strength of the couplings between the amide I modes (which mainly involve the stretching of the  $\text{C}=\text{O}$  bonds of the peptide groups).<sup>2</sup> These coupling strengths are observed as the intensities and anisotropies of the cross-peaks in the 2D vibrational spectrum, and in principle, it might therefore be possible to derive the entire secondary structure of a peptide from its 2D spectrum. In this sense, 2D vibrational spectroscopy is analogous to 2D NMR spectroscopy,<sup>3</sup> but with much better (picosecond) time resolution, and as such it might become a valuable tool in the study of peptide and protein structure and dynamics.

However, to date 2D vibrational spectroscopy has only been used to study peptides with known structure, for which good agreement between observed and calculated 2D spectra was found.<sup>1,4,5</sup> The potential of 2D spectroscopy for structure elucidation has as yet not been demonstrated. Here we present a 2D vibrational study of trialanine in aqueous solution, in which we investigate to what extent the structure of this peptide can be derived from its 2D vibrational spectrum. Recent vibrational circular dichroism studies<sup>6–8</sup> have suggested that trialanine has a stable conformation in aqueous solution. Since trialanine has only two peptide units, the only structure-related degrees of freedom are the two dihedral angles  $\phi$  and  $\psi$  (see Figure 1), which determine the coupling strength  $\beta$  between the two amide I oscillators, and the angle  $\theta$  between their transition dipole vectors.

## II. Experimental Section

Our laser setup consists of a commercial Ti:sapphire amplifier which generates pulses with a duration of 80 fs and an energy of 750  $\mu\text{J}$  (center wavelength 800 nm), part of which (50%) is used to pump a white-light seeded two-stage optical parametric amplifier (OPA) based on BBO.<sup>9</sup> In this way, signal and idler

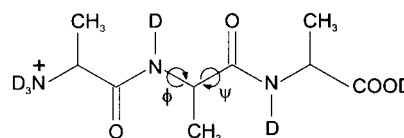


**Figure 1.** Structure of deuterated trialanine at low pD, with the dihedral angles  $\phi, \psi$  indicated by arrows.

pulses tunable from 1.1 to 2.6  $\mu\text{m}$  are generated. Difference-frequency generation of signal and idler in  $\text{AgGaS}_2$  is used to obtain mid-infrared pulses, which are tunable from 2 to 10  $\mu\text{m}$ . The duration of the mid-infrared pulses is 100–150 fs, and at a center frequency of 1650  $\text{cm}^{-1}$  the energy and bandwidth are 1  $\mu\text{J}$  and 200  $\text{cm}^{-1}$ , respectively. A small fraction of the mid-infrared pulses is split off by means of a wedged  $\text{BaF}_2$  window to obtain broadband probe and reference pulses. The remainder, which is used as the pump pulse, is passed through an IR Fabry–Perot filter consisting of two partial reflectors separated by a distance which is regulated by a feedback-controlled piezo-electric mount. In this way, narrow-band pump pulses (bandwidth 11  $\text{cm}^{-1}$ , fwhm  $\sim 750$  fs) are obtained, the center frequency of which can be varied by adjusting the Fabry–Perot filter. In the pump–probe experiments, we use frequency-dispersed detection of the probe and reference pulses by means of a  $2 \times 16$  HgCdTe detector array, which enables us to measure transient spectra on a single-shot basis. Two-dimensional vibrational spectra are obtained by scanning the pump frequency and recording transient spectra for each pump frequency. Scans with either parallel or perpendicularly polarized pump and probe pulses are recorded by adjusting a zero-order  $\lambda/2$  plate placed in the pump beam.

Tri-L-alanine (purity > 99%) was obtained commercially (Bachem Biochemica, GmbH), and was lyophilized from  $\text{D}_2\text{O}$  in order to deuterate the NH groups. The experiments were carried out on 0.15 M solutions of the deuterated trialanine in  $\text{D}_2\text{O}$ , at pD = 1 to ensure that most (>95%) of the carboxylate groups were protonated, thereby minimizing the spectral overlap between the carboxylate CO-stretch and amide I modes. Previous studies have shown no evidence for hydrolysis or aggregation of the peptide under these circumstances.<sup>8,10</sup> The sample was kept between two  $\text{CaF}_2$  windows separated by a 25  $\mu\text{m}$  spacer.

\* To whom correspondence should be addressed. Fax: +49 30 6392 1429. E-mail: hamm@mbi-berlin.de 1.

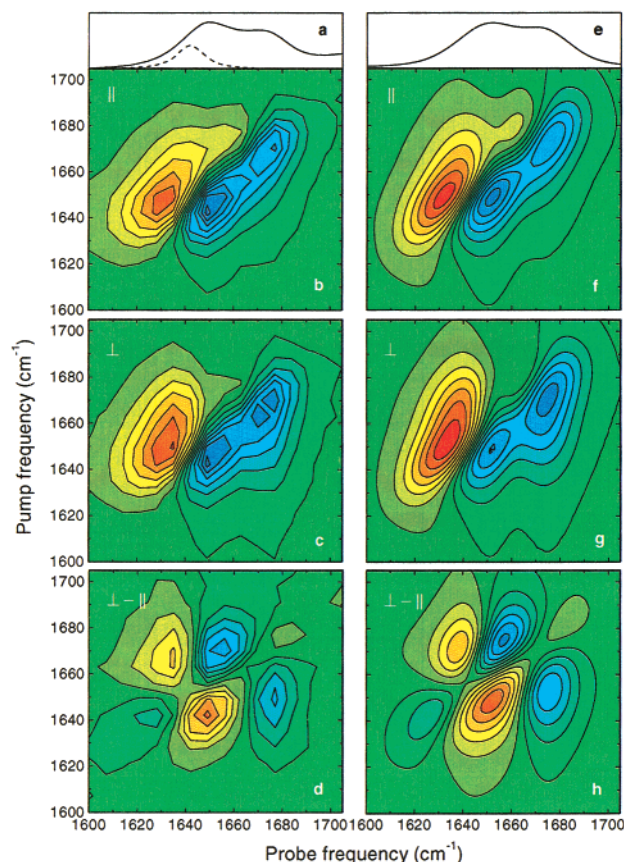


**Figure 2.** (a) Linear absorption spectrum of deuterated trialanine in  $D_2O$  at  $pD = 1$ . The dotted line shows a representative pump-pulse spectrum. (b) 2D spectrum at delay 1.5 ps, for parallel polarizations of the pump and probe pulses, showing the absorption change as a function of pump and probe frequency. Blue colors indicate negative absorption change, red colors positive absorption change. Contour intervals are 0.13 mOD. (c) 2D spectrum for perpendicularly polarized pump and probe. Contour intervals are 0.05 mOD. (d) Difference between perpendicular and parallel signals (both scaled to the maximum value occurring in the respective 2D scans<sup>14</sup>). Contour intervals are 0.04 mOD. (e)–(h) Calculated signals, using parameter values  $\beta = 6 \text{ cm}^{-1}$  and  $\theta = 106^\circ$ . Contour intervals in the 2D plots are the same as those on the left.

### III. Results

Figure 2a shows the linear absorption spectrum of deuterated trialanine in  $D_2O$ . It shows two amide I bands, centered at approximately 1650 and 1675  $\text{cm}^{-1}$ .<sup>6</sup> An additional, weak band is found at approximately 1730  $\text{cm}^{-1}$  (data not shown), which is due to the CO-stretch of the carboxylate group.<sup>11</sup> From 2D vibrational measurements in the 1630–1740  $\text{cm}^{-1}$  frequency region, we found that no significant coupling occurs between the carboxylate CO stretch and the amide I modes.

Figure 2b,c show the 2D pump-probe signal for parallel and perpendicularly polarized pump and probe pulses, respectively. These 2D spectra record the response of the sample as a function of probe frequency and the center frequency of the narrow band pump pulse. When two vibrational modes are coupled, excitation of one gives rise to a spectral change of the other, which is observed as a cross-peak in the off-diagonal region of the 2D spectrum. The 2D spectra were obtained at a delay of 1.5 ps, which is the earliest delay value where on one hand coherent effects due to temporal overlap of pump and probe are negligible, and on the other hand relaxation phenomena do not yet influence the 2D line shape. Along the diagonal of the 2D spectrum one observes the bleach and stimulated emission for

each of the two amide I bands as the negative (blue) signal, and the excited-state absorption as the positive (red) signal at lower probe frequency. The pump-probe signal follows the diagonal, indicating that the amide I bands are inhomogeneously broadened.<sup>12,13</sup>

At first sight, no cross-peak structure can be distinguished in the 2D spectra, mainly because the cross-peaks overlap with the very strong and broad diagonal peaks. This overlap between diagonal and cross-peaks is a problem intrinsic to 2D vibrational spectroscopy on peptides, and is due to the fact that the difference between the uncoupled amide I frequencies is of the same order as the coupling strength and the line width. Here we encounter an important difference between vibrational and NMR 2D spectroscopy: in the latter, the difference between the uncoupled frequencies (chemical shifts) depends linearly on the applied magnetic field, and hence can in principal always be made large compared to the spin coupling and the line width (which are independent of the field strength).

To separate the cross-peaks in the 2D vibrational spectrum from the strong diagonal signal, we exploit their polarization dependence. The pumped and probed transition dipoles giving rise to the cross-peak signal are in general not parallel, which renders the anisotropy of the cross-peaks different from that of the diagonal peaks (which is ideally  $2/5$ ). Hence, by subtracting the parallel from the perpendicular scan (both scaled to the maximum occurring on their respective diagonals<sup>14</sup>) the diagonal peaks are eliminated, and the cross-peaks clearly revealed (Figure 2d). The cross-peaks arise from the coupling between the two amide I modes, which, in first-order approximation, causes an anharmonic frequency-shift of the one when the other is populated. As a consequence, each cross-peak has a dispersive shape along the probe direction, with a negative (bleach) and positive (excited-state absorption) contribution.

### IV. Discussion

To interpret our data we use an excitonic model for the amide I band, which has been described in detail elsewhere.<sup>4,15</sup> This model has been successful in describing both the linear<sup>16,17</sup> and third-order nonlinear<sup>1,4,5</sup> response of the amide I band of peptides and proteins. No assumptions concerning the coupling between the amide I modes are made, except that it is bilinear in the displacement coordinates of the two coupled modes. We use the eigenstates of the noninteracting peptide groups (site states) as a basis set. In this basis, the coupling gives rise to off-diagonal contributions in both the one- and two-exciton Hamiltonian. If the site basis set is ordered as  $\{|0,0\rangle, |1,0\rangle, |0,1\rangle, |2,0\rangle, |0,2\rangle, |1,1\rangle\}$ , where  $|m,n\rangle$  denotes the state in which the first and second peptide group have  $m$  and  $n$  vibrational quanta, respectively, then the Hamiltonian is represented by<sup>4</sup>

$$H = \begin{pmatrix} 0 & & & & & \\ & \epsilon_1 & \beta & & & \\ & \beta & \epsilon_2 & & & \\ & & & 2\epsilon_1 - \Delta & 0 & \sqrt{2}\beta \\ & & & 0 & 2\epsilon_2 - \Delta & \sqrt{2}\beta \\ & & & \sqrt{2}\beta & \sqrt{2}\beta & \epsilon_1 + \epsilon_2 \end{pmatrix} \quad (1)$$

where the zero-, one-, and two-exciton manifolds have been separated by lines. In this matrix,  $\epsilon_1$  and  $\epsilon_2$  are the amide I frequencies in absence of coupling,  $\beta$  the coupling strength, and  $\Delta$  the anharmonicity. The factor  $\sqrt{2}$  in the coupling between the two-exciton states originates from a harmonic approximation.<sup>4</sup> Note that there is no coupling between the manifolds,

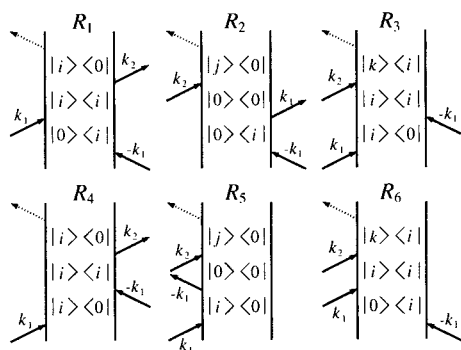


**Figure 3.** Double-sided Feynman diagrams needed to describe the pump–probe response in the present experiment. The indexes  $i, j$  run over the one-exciton states, the index  $k$  over the two-exciton states. The pump and probe wave vectors are  $k_1$  and  $k_2$ , respectively.

which indicates that the number of excitons is still a good quantum number. The transition dipole vectors  $\mu_{|0,0\rangle \rightarrow |1,0\rangle}$  and  $\mu_{|0,0\rangle \rightarrow |0,1\rangle}$  of the site states are at an angle which we define as  $\theta$ . In the harmonic approximation we have  $\mu_{|1,0\rangle \rightarrow |2,0\rangle} = \sqrt{2}\mu_{|0,0\rangle \rightarrow |1,0\rangle}$  and  $\mu_{|0,1\rangle \rightarrow |0,2\rangle} = \sqrt{2}\mu_{|0,0\rangle \rightarrow |0,1\rangle}$ .

By diagonalization of the Hamiltonian (1) one finds the one- and two-exciton energies  $\Omega_i^{(1)}$  and  $\Omega_i^{(2)}$  and the excitonic eigenstates, the latter being linear combinations of the site states. The transition dipoles of the exciton states are obtained from the transition dipole matrix in the site basis by means of the appropriate unitary transformation. Note that the angle between the transition dipole vectors of the excitonic states and the angle  $\theta$  between the uncoupled amide I modes are not necessarily equal. Using the exciton energies and exciton transition dipoles the pump–probe signal can be calculated. In our calculation we only take sequential (pump–pump–probe) interactions of the exciton system with the electromagnetic field into account. We find that the Liouville-space pathways in which the pump pulse excites a coherent superposition of two excitons (i.e., in which the system is in a coherence state  $|i\rangle\langle j|$  after the second interaction with the pump pulse) contribute negligibly (less than 1%) to the pump–probe signal since the bandwidth of the pump pulses is smaller than the splitting of the one-excitonic states. Hence, only the Feynman diagrams shown in Figure 3 have to be taken into account. These diagrams represent the stimulated emission ( $R_1 + R_4$ ), bleach ( $R_2 + R_5$ ), and excited-state absorption ( $R_3 + R_6$ ) contributions to the pump–probe signal, respectively. The corresponding response functions can be derived directly from these Feynman diagrams, and are given by

$$R_1 + R_4 = \sum_i \langle \mu_{0i} \mu_{0i} \mu_{0i} \mu_{0i} \rangle e^{-i\Omega_i^{(1)}t_3} \cos(\Omega_i^{(1)}t_1) e^{-\gamma_2(t_1+t_3)} \quad (2)$$

$$R_2 + R_5 = \sum_{i,j} \langle \mu_{0i} \mu_{0j} \mu_{0i} \mu_{0j} \rangle e^{-i\Omega_j^{(1)}t_3} \cos(\Omega_i^{(1)}t_1) e^{-\gamma_2(t_1+t_3)} \quad (3)$$

$$R_3 + R_6 = - \sum_{i,k} \langle \mu_{ik} \mu_{ik} \mu_{0i} \mu_{0i} \rangle e^{-i(\Omega_k^{(2)} - \Omega_i^{(1)})t_3} \times \cos(\Omega_i^{(1)}t_1) e^{-\gamma_2(t_1+t_3)} \quad (4)$$

where  $\gamma_2 = 1/T_2$ . The indices  $i, j$  run over the one-exciton states and the index  $k$  over the two-exciton states (see Figure 3), and the dipole vectors of the  $0 \rightarrow 1$  and  $1 \rightarrow 2$  exciton transitions are denoted by  $\mu_{0i}$  and  $\mu_{ik}$ . The bracket  $\langle \dots \rangle$  denotes an average over all molecular orientations. Since the exciton energies depend on  $\beta$ , and the exciton transition dipoles on  $\theta$ , the above response functions depend on these structural parameters as well.

The response functions, which contain products of four vectors, are tensors of fourth rank. For the pump–probe experiments discussed here, in which the first and second interactions are always with the pump, and the third and fourth interactions always with the probe field, only the  $xxxx$  and  $yyxx$  components, which represent parallel and perpendicularly polarized pump and probe fields respectively, are relevant. These components can be calculated using the orientational averages of the appropriate direction cosines,<sup>18</sup> and are given by

$$\langle (\mu' \cdot \mathbf{e}_x)(\mu' \cdot \mathbf{e}_x)(\mu \cdot \mathbf{e}_x)(\mu \cdot \mathbf{e}_x) \rangle = \frac{1}{15}(|\mu'|^2|\mu|^2 + 2(\mu' \cdot \mu)^2) \quad (5)$$

$$\langle (\mu' \cdot \mathbf{e}_y)(\mu' \cdot \mathbf{e}_y)(\mu \cdot \mathbf{e}_x)(\mu \cdot \mathbf{e}_x) \rangle = \frac{1}{15}(2|\mu'|^2|\mu|^2 - (\mu' \cdot \mu)^2) \quad (6)$$

where  $\mathbf{e}_x$  and  $\mathbf{e}_y$  are unit vectors in the  $x$  and  $y$  directions.

The frequency dispersed pump–probe signal is calculated using the response functions and the envelope functions of the pump and probe pulses.<sup>19</sup> We assume a single sided exponential shape for the pump pulse intensity, and a delta function for the probe pulse. For the anharmonicity  $\Delta$  of the amide I mode we use the previously determined value of  $16 \text{ cm}^{-1}$ .<sup>4</sup> As already stated, the 2D pump–probe signal follows the diagonal, which means the amide I band is inhomogeneously broadened.<sup>13</sup> To incorporate this inhomogeneity in the calculation, we assume the same homogeneous line width for both amide I modes, and uncorrelated Gaussian inhomogeneous distributions for the site frequencies  $\epsilon_1$  and  $\epsilon_2$ . The assumption of uncorrelated site frequencies is justified for the present system, in which the two peptide units are highly exposed to the surrounding solvent. The total pump–probe signal is calculated by numerically integrating over these inhomogeneous distributions, diagonalizing the Hamiltonian (1) and calculating the pump–probe signal using (2–4) for each pair of site frequencies  $\epsilon_1, \epsilon_2$ .

Figure 2e–h show the result of a simultaneous least-squares fit of calculated pump–probe signals to both the parallel and perpendicular experimental 2D signals. This least-squares fit involves six parameters: the two site frequencies (i.e., the center frequencies of the respective inhomogeneous distributions), the homogeneous and inhomogeneous line widths, the coupling strength  $\beta$ , and the angle  $\theta$  between the dipole vectors of the uncoupled amide I modes. Of these parameters, the site frequencies and the homogeneous and inhomogeneous line widths mainly determine the diagonal part of the 2D signal, whereas the coupling strength  $\beta$  and the angle  $\theta$  mainly determine the off-diagonal part and its anisotropy. From the least-squares fit, we obtain  $\beta = 6 \text{ cm}^{-1}$  for the coupling strength, and  $\theta = 106^\circ$  for the angle between the transition dipole vectors.<sup>20</sup> It should be noted that since both the pump–probe signal and the linear absorption spectrum are invariant under the transformation  $(\beta, \theta) \rightarrow (-\beta, 180^\circ - \theta)$ , our measurements imply either  $(\beta, \theta) = (6 \text{ cm}^{-1}, 106^\circ)$  or  $(\beta, \theta) = (-6 \text{ cm}^{-1}, 74^\circ)$ . The value of the coupling strength  $\beta$  is small compared to the splitting of the two amide I frequencies, indicating that the interpeptide coupling is in the weak coupling limit, where the vibrational excitons are localized mainly on either of the two peptide groups.

The values of  $\beta$  and  $\theta$  are determined by the secondary peptide structure, and since the peptide ( $-\text{CO}-\text{ND}-$ ) group is essentially planar,<sup>21</sup> by the two dihedral angles  $\phi$  and  $\psi$  only (see Figure 1). Hence, if the functional relation between  $(\beta, \theta)$  and  $(\phi, \psi)$  is known, the value of the latter, and hence the structure of the peptide backbone, can be derived from the experimentally determined  $\beta$  and  $\theta$ . To determine this functional



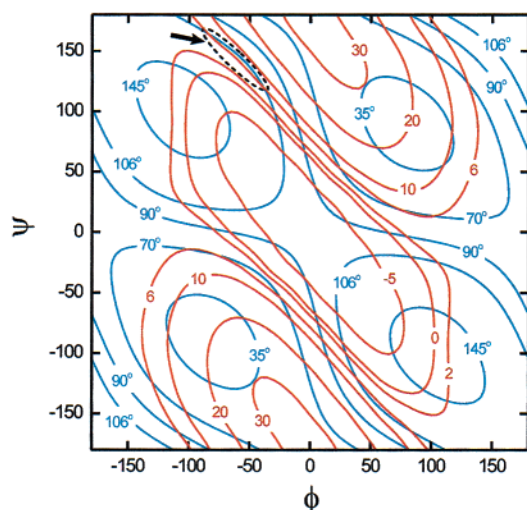


**Figure 4.** Calculated coupling strength  $\beta$  (in  $\text{cm}^{-1}$ , red contours), kindly provided to us by the authors of ref 22, and angle  $\theta$  (in degrees, blue contours) between the two amide I transition dipoles as a function of the dihedral angles  $\theta$  and  $\psi$ , which are defined as shown in Figure 1.

relation, we have used the results of an *ab initio* molecular orbital calculation of the coupling strength as a function of  $(\phi, \psi)$  in a system consisting of two covalently bonded peptide groups, which was recently reported by Torii and Tasumi.<sup>22</sup> The results of this calculation, which was carried out on the HF level using an augmented 6-31G\*\* basis set, were kindly provided to us by the authors. Since this is a quantum-chemical calculation, it includes the through-space electrostatic interaction exactly, avoiding the limitations of the dipole approximation. It also takes into account through-bond exchange interaction due to overlap of the electronic orbitals. It does however neglect kinematic coupling through the  $\text{C}^\alpha$  group, since the nuclear displacements of the amide I eigenmodes are assumed to be localized on the  $\text{CO-NH}$  unit.<sup>22</sup> The angle  $\theta$  between the two transition dipoles was calculated for all possible values  $(\phi, \psi)$ , assuming an angle of  $20^\circ$  between the  $\text{C}=\text{O}$  axis and the transition dipole.<sup>2</sup> In Figure 4, the coupling strength  $\beta$  (red contours) and the angle  $\theta$  (blue contours) are plotted as a function of  $(\phi, \psi)$ .

Using the contour graph of Figure 4, the structure of the peptide can be determined directly from the experimentally determined  $\beta$  and  $\theta$ , simply by finding the  $(\phi, \psi)$  coordinates of the points where the  $\beta = 6 \text{ cm}^{-1}$  and  $\theta = 106^\circ$  contours or the  $\beta = -6 \text{ cm}^{-1}$  and  $\theta = 74^\circ$  contours intersect. There are two regions where this occurs,  $(\phi, \psi) \approx (-60^\circ, 140^\circ)$  and  $(\phi, \psi) \approx (60^\circ, -140^\circ)$ , situated center-symmetrically in the Ramachandran plot. Because of sterical hindrance by the residual methyl group of L-alanine,<sup>21</sup> only the region at  $(-60^\circ, 140^\circ)$  (indicated by the arrow in Figure 4) corresponds to a physically realizable structure. In this conformation, the two  $\text{C}=\text{O}$  groups form a left-handed structure, in agreement with the sign of the couplet observed in vibrational circular dichroism (VCD) spectroscopy.<sup>6</sup> Note that this can be concluded without specifically assigning the two amide I states to the peptide units.

It is well established that peptide conformations generally occur in two regions of the  $(\phi, \psi)$  conformational space.<sup>21</sup> The first region, around  $(\phi, \psi) = (-60^\circ, -50^\circ)$ , is typical for the right-handed  $\alpha$ -helix and (with slightly different dihedral angles) the  $\pi$ - and  $3_{10}$ -helix. The second region corresponds to secondary structures such as the antiparallel  $\beta$ -sheet ( $-139^\circ, 135^\circ$ ), the parallel  $\beta$ -sheet ( $-119^\circ, 113^\circ$ ), and the poly(Gly) II structure ( $-80^\circ, 150^\circ$ ), the latter of which is very close to the structure derived from the present experiment.

Vibrational circular dichroism studies have concluded that trialanine in aqueous solution adapts mainly one conformation, although its structure could not be derived.<sup>6–8</sup> On the other hand, NMR studies on terminally blocked alanine (*N*-acetyl-L-alanine-*N*-methyl amide), the central structure of which is identical to that of trialanine, have concluded that for this molecule there exists a distribution of conformers.<sup>23</sup> Although from our measurements alone it cannot be concluded with certainty that trialanine adapts only one conformation, this does seem probable for two reasons. First, if several conformers occur, the observed  $\beta$  and  $\theta$  would be accordingly weighted averages. Since the functional relation between  $(\phi, \psi)$  and  $(\beta, \theta)$  is highly nonlinear, the averaged values of  $\beta$  and  $\theta$  would in general not correspond to a meaningful structure. The observed  $\beta$  and  $\theta$  do however correspond to a physically meaningful conformation, namely, the poly(Gly) II structure which is known as one of the stable conformations.<sup>24–27</sup> Second, the angle  $\theta$ , and therewith the cross-peak anisotropy  $r = 1/5(3 \cos^2 \theta - 1)$ ,<sup>1</sup> is close to its extreme value of  $90^\circ$  (note that  $\theta$  and  $180^\circ - \theta$  yield the same cross-peak anisotropy). Hence, if there would be a distribution of conformers, only those having  $\theta$  very close to  $90^\circ$  could contribute significantly. While this is the case for the poly(Gly) II structure, the  $\alpha$ -helical-like structures have rather small angles ( $\theta \leq 50^\circ$ ), so that the contribution from this region of the conformational space would have to be small.

Interestingly, several molecular dynamics (MD) simulations<sup>24,27</sup> have shown that for terminally blocked alanine, the  $\beta$ -sheet/poly(Gly) II conformation has a free energy approximately  $500 \text{ cm}^{-1}$  below that of the  $\alpha$ -conformation, which would confirm that the former conformation is predominant. However, other MD studies have reported different values for the depth of the free-energy minima of the two conformations,<sup>25,26</sup> the disagreement being mainly due to the different force fields employed, and the exact values remain to be settled. We hope the results presented here will stimulate further work in this direction.

## V. Conclusions

The above results show that a substantial amount of structural information can be derived from the two-dimensional vibrational spectra of small peptides in solution. In particular, we have derived a distinct prediction for the backbone structure of trialanine in aqueous solution from its 2D vibrational spectrum. It is also clear that the full potential of 2D vibrational spectroscopy is only realized when quantum-chemical calculations are employed in the interpretation of the data.<sup>22</sup> Finally, we have presented a method for revealing the cross-peak structure in congested 2D vibrational spectra by using the anisotropy difference between diagonal and cross-peaks. This method may also be of use in 2D spectroscopy on larger peptides, where the overlap of the diagonal and cross-peaks will certainly also occur.

**Acknowledgment.** We gratefully acknowledge H. Torii and M. Tasumi for providing us with the results of their calculations. We acknowledge financial support by the Deutsche Forschungsgemeinschaft (DFG). We thank Thomas Elsaesser for critically reading the manuscript and his continuous support of the project.

## References and Notes

- (1) Hamm, P.; Lim, M.; DeGrado, W. F.; Hochstrasser, R. M. *Proc. Natl. Acad. Sci. U.S.A.* **1999**, *96*, 2036.
- (2) Krimm, S.; Bandekar, J. *Adv. Protein Chem.* **1986**, *38*, 181.

- (3) Ernst, R. R.; Bodenhausen, G.; Wokaun, A. *Principles of Nuclear Magnetic Resonance in One and Two Dimensions*; Clarendon Press: Oxford, 1987.
- (4) Hamm, P.; Lim, M.; Hochstrasser, R. M. *J. Phys. Chem. B* **1998**, *102*, 6123.
- (5) Hamm, P.; Lim, M.; DeGrado, W. F.; Hochstrasser, R. M. *J. Chem. Phys.* **2000**, *112*, 1907.
- (6) Lee, O.; Roberts, M.; Diem, M. *Biopolymers* **1989**, *28*, 1759.
- (7) Zuk, W. M.; Freedman, T. B.; Nafie, L. A. *Biopolymers* **1989**, *28*, 2025.
- (8) Ford, S. J.; Wen, Z. Q.; Hecht, L.; Barron, L. D. *Biopolymers* **1994**, *34*, 303.
- (9) Hamm, P.; Lim, M.; Hochstrasser, R. M. *J. Chem. Phys.* **1997**, *107*, 10523.
- (10) Koçak, A.; Luque, R.; Diem, M. *Biopolymers* **1998**, *46*, 455.
- (11) Sieler, G.; Schweitzer-Stenner, R.; Holtz, J. S. W.; Pajcini, V.; Asher, S. A. *J. Phys. Chem. B* **1999**, *103*, 372.
- (12) Hybl, J. D.; Albrecht, A. W.; Faeder, S. M. G.; Jonas, D. M. *Chem. Phys. Lett.* **1998**, *297*, 307.
- (13) Tokmakoff, A.; *J. Phys. Chem. A* **2000**, *104*, 4247.
- (14) The ratio of the parallel and perpendicular scaling factors is 2.30 both in the experimental and calculated 2D plots. This is slightly less than the ideal value of 3, probably because overlap of the diagonal and cross-peaks causes a slight decrease of the diagonal peak, which is different for parallel and perpendicular polarizations.
- (15) Piryatinski, A.; Tretiak, S.; Chernyak, V.; Mukamel, S. *J. Raman Spectrosc.* **2000**, *31*, 125.
- (16) Torii, H.; Tasumi, M. *J. Chem. Phys.* **1992**, *96*, 3379.
- (17) Torii, H.; Tasumi, M. In *Infrared Spectroscopy of Biomolecules*; Mantsch, H. H., Chapman, D., Eds.; Wiley-Liss: New York, 1996; Chapter 1.
- (18) Bright Wilson, E., Jr.; Decius, J. C.; Cross, P. C. *Molecular Vibrations*; McGraw-Hill: New York, 1955.
- (19) Mukamel, S. *Principles of Nonlinear Optical Spectroscopy*; Oxford University Press: Oxford, 1995.
- (20) The uncertainty in these parameter values is difficult to estimate because of systematical errors. However, we find that changing  $\theta$  by  $10^\circ$  and fitting again (keeping  $\theta$  fixed) results in a significantly worse agreement between calculation and experiment, especially in the off-diagonal region of the 2D scans. The same holds for changing  $\beta$  by  $1\text{ cm}^{-1}$ .
- (21) Creighton, T. E. *Proteins*; W. H. Freeman and Company: New York, 1993.
- (22) Torii, H.; Tasumi, M. *J. Raman Spectrosc.* **1998**, *29*, 81.
- (23) Madison, V.; Kopple, K. D. *J. Am. Chem. Soc.* **1980**, *102*, 4855.
- (24) Anderson, A. G.; Hermans, J. *Proteins* **1988**, *3*, 262.
- (25) Brooks, C. L., III.; Case, D. A. *Chem. Rev.* **1993**, *93*, 2487.
- (26) Smith, P. E.; *J. Chem. Phys.* **1999**, *111*, 5568.
- (27) Apostolakis, J.; Ferrara, P.; Caflish, A. *J. Chem. Phys.* **1999**, *110*, 2099.